Egypt. J. Chem. **Vol. 67,** No. 6 pp. 337 - 344 (2024)

Egyptian Journal of Chemistry

http://ejchem.journals.ekb.eg/

Novel and effective pyrimidone derivative adsorbent for adsorptive removal of cationic methylene blue dye: isotherm, kinetic and thermodynamic studies.

Manojkumar Rajapriyan[a], Imran khan R[b], Meera Moydeen A[c], Badr M. Thamer[c], Abdulwahab Salah[d] and Syed Ali Padusha M[a]*

[a*]*PG & Research Department of Chemistry, Jamal Mohamed College, Affiliated to Bharathidasan University, Tiruchirappalli, Tamilnadu – 620 020, India.*

[b]*National Postdoctoral Fellow, Department of Organic Chemistry, Indian Institute of Science, Bangalore, Karnataka – 560 012, India.*

[c]*Department of Chemistry, College of Science, King Saud University, Riyadh 11451, Saudi Arabia.*

[d]*Faculty of Chemistry, National and Local United Engineering Laboratory for Power Batteries Northeast Normal University, Changchun, 130024, China.*

Abstract

Adsorbents based on carbonaceous materials, polymers, clays, and inorganic materials are common in the literature, but adsorbents designed from organic materials such as self-assembled heterocyclic compounds have not been studied so far. In this study, a new adsorbent pyrimidone derivative (DHPM) was synthesised employing a green protocol to tone down the cationic dye Methylene Blue (MB) from aqueous solution. The synthesised self-assembled bio-inspired molecules is characterized using Ultraviolet Spectroscopy (UV-Vis), Fourier transform infrared (FT-IR), ^{1}H NMR & ^{13}C NMR and Thermogravimetric analysis (TGA). The self-assembled molecule's propensity to adsorb MB dye was investigated as a function of MB concentration, time, temperature, pH and adsorbent dosage. The enhancement of adsorption capability over the cationic dye has been discussed in this script. A detailed examination of the adsorption kinetics revealed that the study conforms to pseudo-second-order model. Isothermal adsorption study over the MB dye were used with several models. Langmuir-Freundlich model was found to be the most accurate, with an adsorption capacity of 233.99 mg/g. The results are endothermic and spontaneous for the thermodynamic study of adsorption over MB dye onto the pyrimidone derivative.

Keywords: Pyrimidone derivative (DHPM), Adsorption, Methylene blue, Isotherm, Kinetic.

1. Introduction

Among all other synthetic dyes, Methylene blue (MB) a heterocyclic aromatic compound, is frequently used than any other synthetic dyes in chemical and biological disciplines. This odourless dark green solid powder produces a blue-coloured solution when it combines in aqueous medium [1,2]. More frequently, MB is predominantly utilised for paper colouring, temporary hair colouring, and colouring cotton and wool as a colouring agent. However, MB's adverse effects can exacerbate vision impairment, and repeated inhalation may result in nausea, vomiting, and mental illness [3,4]. Stopping the excessive release of dangerous substances into water bodies will protect the environment and the present bio cycle [5-15].

There are several methods to manage dye wastewater, including oxidative degradation, membrane separation, flocculation, sedimentation and adsorption [16-24]. It is challenging to popularise and deploy on a big scale despite the fact that they frequently need high costs and intricate operations [25,26]. Adsorption technology is currently the preferred method for removing dyes, and it is opted by researchers due to its ease of utilizing, safety, high efficiency, economy, multiple applications, and so on [27-29]. Target compounds can be specifically removed from complex pollutant solutions by adsorption technique because of it is selectivity [30-33].

Since, the self-assembled bio-inspired molecules are an effective approach to build nano/micro-architectures, with several applications, particularly in the fields of biomedical sciences, bio-sensing, tissue engineering, etc., [34,35]. Such self-assembling processes are typically propelled by non-covalent interactions between the relevant moieties, including hydrogen bonds, hydrophobic forces, electrostatic interactions, π– π* stacking, and non-specific van der Waals forces [36]. The self-assembly of tiny organic molecules into various structural motifs has sparked tremendous interest for the adsorption investigation, which is motivated by its various applications created by the architectures of natural building blocks [37]. Although, carbon has a wide range of applications, it has not yet been used as an adsorbent to remove pollutants from polluted water. There are many materials used as an adsorbent in this work before, but this organic material has high efficiency of bond making ability with the MB dye. Further, self-assembled heterocyclic

*Corresponding author e-mail: sp@jmc.edu.; (M. Syed Ali Padusha).

Receive Date: 11 November 2023, Revise Date: 04 December 2023, Accept Date: 11 December 2023

DOI: 10.21608/EJCHEM.2023.247903.8849

compounds have a wide range of applications, they also have not yet been used as an adsorbent to remove pollutants from polluted water.

In this work, a self-assembled heterocyclic molecule Ethyl 4-(2,4-dimethoxyphenyl)-6-methyl-2-oxo-1,2,3,4-tetrahydropyrimidine-5-carboxylate (DHPM) with attractive physicochemical properties was synthesized by the environmentally benign techniques and it was utilized as novel adsorbent for removal of cationic MB dye. The characterization techniques like Fourier transform infrared (FT-IR), ^{1}H NMR & ^{13}C NMR and Thermogravimetric analysis (TGA) were analysed to evaluate the structure and physical nature of the self-assembled molecule. The adsorption capacity of the synthetic DHPM derivative was evaluated on toning down the MB dye from an aqueous solution. In diverse experimental settings, a variety of isotherm and kinetics models were used to assess the way the MB dye behaved upon being removed from polluted water.

2. Materials and Methods

Aerobic conditions were used for all reactions. Unless otherwise stated, the chemicals purchased were used without additional purifications which are procured from Sigma Aldrich.

2.1 Synthesis of Ethyl 4-(2,4-dimethoxyphenyl)-6-methyl-2-oxo-1,2,3,4-tetrahydropyrimidine-5-carboxylate (DHPM)

2,4-dimethoxy-benzaldehyde (1 mmol), Ethyl-acetoacetate (1 mmol) and urea (1 mmol) were added (Fig. 1). The mixture was then stirred for 30 min at room temperature. TLC was used to ensure the completion of the reaction with ethyl acetate and n-hexane (1:4) as the eluent system. After this process, the mixture was added twice with ethyl acetate (2 x 20 ml) for the extraction. The extracted organic layer was concentrated, washed twice with distilled water and dried over anhydrous Na_2SO_4. The resulting solid was recrystallized with ethyl acetate. The yellow colour solid with yield of 95% was noted.

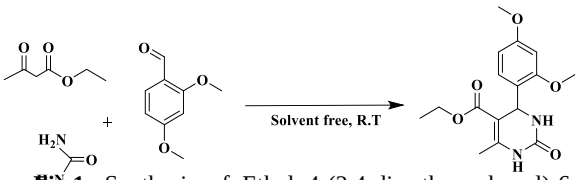

Fig.1: Synthesis of Ethyl 4-(2,4-dimethoxyphenyl)-6-methyl-2-oxo-1,2,3,4-tetrahydropyrimidine-5-carboxylate (DHPM).

2.2 Characterization

On a Bruker spectrometer, NMR spectra were recorded at 400 MHz using DMSOd_6 solvent and TMS as the internal standard. A BRUKER ALPHA II ECO-ATR instrument was used to measure the FT-IR spectrum from 4000–550 cm^{-1} range and Thermo Gravimetric Analyzer (TGA 4000 – PerkinElmer) were used.

2.3 Adsorption Study

The batch studies were carried out by a process of varying the concentrations between 25 to 200 mg L−1 (25, 50, 75, 100, 150, and 200 mg L−1). A 50 mL Erlenmeyer flask is filled with 10 mL of MB dye solution and 10 mg of adsorbent (DHPM). The flask was tend to shake in a thermostat shaker-water bath at 298 K for 24 h, and the same were stirred at 70 rpm. By varying the dye solution's pH (50 mg L−1) in various ranges between 2.5–10, the effect of pH on MB adsorption was investigated. 0.1 M HCl or NaOH solutions were used to alter the pH in order to attain the desired pH of the MB dye solution. To determine the impact of temperature, a 10 mL of the MB solutions with 10 mg of adsorbent (DHPM) was kept at an initial concentration of 50 mg L−1 and tested by ascending the temperature from 298, 303, 308, and 313 K for 24 h. The dye solution of 0.1 mL was taken from the top of the tube and diluted to 3 mL for measuring the dye's residual concentration. To quantify the absorbance, a UV-Vis spectrophotometer (UV–Vis) was used at λmax = 664 nm. At a concentration of 50 mg L^{-1} by adding 100 mg of DHPM with 100 mL of pH 10 MB dye solution was agitated at 298 K to evaluate the kinetic studies. During agitation, at regular intervals (from 6 min to 24 h) the MB solution was measured for the absorbance using UV-Vis spectroscopy at λmax = 664 nm. The following equations (1-2) were used to determine the quantity of MB adsorbed on DHPMs at equilibrium (qe, mg g^{-1}) and at time t (qt, mg g^{-1}) as well as removal efficiency.

$$q_e = \frac{C_o - C_e}{m} \times V$$

$$q_t = \frac{C_o - C_t}{m} \times V$$

3. Results

3.1 Characterization of DHPMs

The FT-IR spectrum (Fig. 2) of DHPMs shows the presence of an NH which is ensured by 3237 cm^{-1} band appearance. Further, the aromatic C=O presence is confirmed by the existence of a 1696 cm^{-1} band. A band at 1076 cm^{-1} confirms the existence of C-N-C.

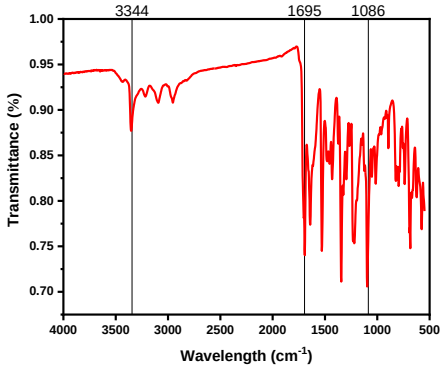

Fig. 2. The FT-IR spectrum of DHPMs

Proton NMR confirms the structure of DHPMs shown [38] in Fig 3a. ^{1}H NMR (400 MHz, DMSO-d6): δH (ppm) 9.05 (s, 1H, NH), 7.16 (s, 1H, NH), 6.94−6.42 (m, 5H, Ar−H), 5.40 (d, 1H), 3.92−3.90 (q, 2H), 3.32 (s, 3H), 1.06−1.02 (t, 3H); 13C NMR peaks in Fig 3b refers the carbon present in the DHPMs. ^{13}C NMR (400 MHz, DMSO-d6): δC (ppm) 14.52, 18.59, 49.00, 59.43, 98.90, 124.66, 128.22, 148.98, 152.73, 158.01, 165.87.

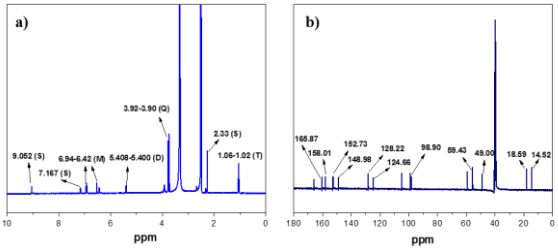

Fig. 3. a) ^{1}H NMR spectrum of DHPMs & b) ^{13}C NMR spectrum of DHPMs

Thermogravimetric analysis was used to investigate the thermal of stability and purity of synthesized DHPM molecules. TGA-DTG image shows the single step degradation at 300 – 380 ºC around 80 % which could be due to the decarboxylation and complete decomposition of amino groups (Fig. 4a). The residual content of the sample was calculated at 700 ºC around 12 % which could be the remaining carbon from the molecule. DSC thermogram shows the Tm around 218 ºC with sharp endothermic peak (Fig. 4b).

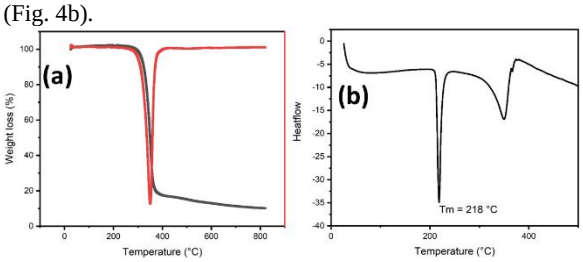

Fig. 4. (a) TGA/DTA analysis (b) DSC analysis of DHPM.

3.2 Adsorption performance

The role of pH in adsorption processes cannot be overstated, as it can significantly affect the interactions between dyes and adsorbents. To determine the impact of pH on adsorption of MB (Fig. 5a), the solution pH values were adjusted between 4.0 to 10. The adsorbent's capacity for adsorption increased steadily as the pH increased from 3.0 to 5.0 at initial. However, it decreased between pH 5.0 and 9.0, and then increased again at pH higher than 9.0. The highest adsorption capacity was recorded at pH 10, with values of 57.77 mg/g. This can be an imputation of the ionization of –C=O and –NH– groups on the adsorbent surface at higher pH, creating more active adsorption sites for MB dye molecules and enhancing electrostatic interaction between positively charged MB dye and the adsorbent surface. Based on the previously mentioned findings, pH 10 was chosen for the MB adsorption studies.

The adsorption capacity for the initial MB dye concentrations was examined by conducting experiments using concentrations between 25 and 400 mg/L. The results depicted in Fig. 5b reveals the capability of adsorption on MB dye increases when initial concentration increases, which could be attributed to the greater concentration gradient pressure generated by higher initial concentrations. The mass transfer of MB molecules from the solution to the surface of the adsorbent would be aided by the driving forces [39]. It ought to be noted that, the adsorption site on adsorbent's surface attain entire saturation at a concentration of 300 mg/L.

For optimising the process of adsorption, it requires a study on the effect of temperature on dye adsorption. It was found that the adsorption capability increases from 19.67 to 35.69 mg/g with rise in temperature from 25 to 50 ºC (Fig. 5c). At higher temperatures, the kinetic energy of the dye molecules increases, which facilitates their diffusion and adsorption onto the adsorbent surface. Also, the solubility of the dye in water decreases with increasing temperature, which results in a higher concentration of the dye in the adsorption layer.

The contact time for effective dye removal is a crucial factor to consider when using adsorbent in wastewater treatment. To evaluate the adsorption capability for MB dye removal at 100 mg/L, the experiments were conducted at 25^0C for varying durations, as shown in Fig. 5d. The adsorption capability for MB dye increased with increasing in contact time. Specifically, adsorption equilibrium was achieved after 150 min.

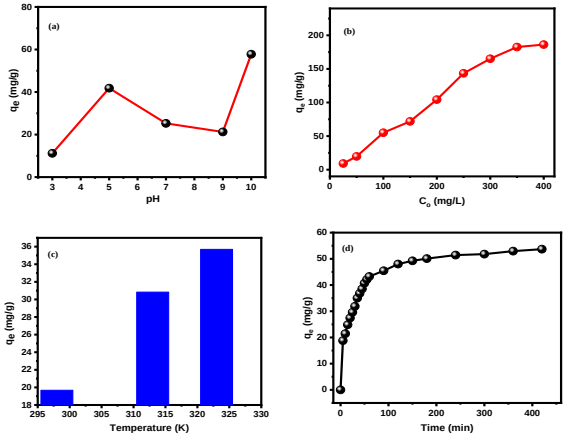

Fig 5. Effect various parameters on adsorption MB onto DHPM adsorbent (a) pH, (b) initial concentration of MB, (c) temperature and (d) contact time.

3.2.1. Isotherm study

To determine the maximum adsorption capacity and to understand the sorption interaction, adsorption isotherms were used. Langmuir [40], Freundlich [41], Dubinin-Radushkevich [42] and Langmuir-Freundlich isotherm [43] models were plotted. The isotherm models of adsorption for the MB adsorption using the DHPM as the adsorbent were nonlinearly fitted and the results were shown in Fig. 6 with the corresponding parameters were calculated from these plots are presented in Table 1. Among the models, Langmuir-Freundlich isotherm model exhibited the highest R2 and lowest chi square ($\chi 2$), indicating its suitability in explaining the process of adsorption. According to this model, the maximum adsorption capability (Qmax) for MB dye at room temperature (298 K) was found to be 233.99 mg/g. Table 1 also illustrates that the RL values for adsorbent were greater than 0.55066 and less than one, indicating that the adsorption process was favourable. Dubinin-Radushkevich model was used to calculate the mean energy (E), which provides valuable insights into the adsorption mechanism. A low value of E, which is below 8 kJ/mol, suggests physical adsorption, while a high value indicates chemical adsorption [44]. The results of this study reveal that the adsorption process was physical, as the E value was 0.02486 kJ/mol.

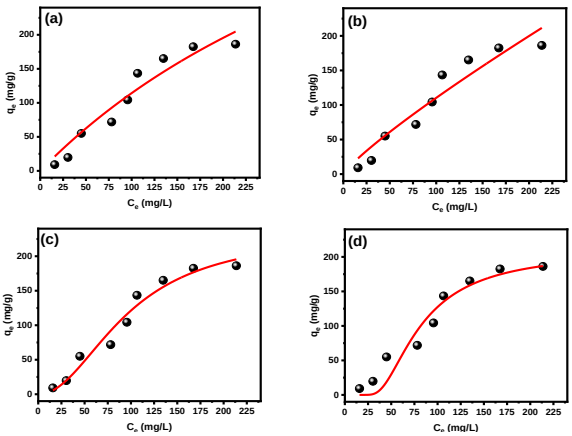

Fig 6. Nonlinear isotherm plot for the adsorption of MB on the DHPM (a) Langmuir, (b) Freundlich (c) Langmuir-Freundlich and (d) Dubinin-Radushkevich model.

Table 1. Equations and parameters of isotherm models for adsorption MB onto DHPM adsorbent.

Model	Parameter value	Equation
Langmuir		
$Q°_{max}$	674.73	$q_e = \frac{Q_o K_L C_e}{1 + K_L C_e}$
K_L	0.00204	
R_L (C_o: 25 to 400 mg/L)	0.95147 to 0.55066	$R_L = \frac{1}{1 + K_L C_o}$
R^2	0.9371	
χ^2	339.35	
Freundlich		
K_F	2.13	
n	1.16	$q_e = K_f\, C_e^{1/n}$
R^2	0.92349	
χ^2	412.77	
Langmuir-Freundlich		
$Q°_{max}$	233.99	
$K_{L\text{-}F}$	0.01036	$q_e = \frac{Q_o (K_{LF} C_e)^m}{1 + (K_{LF} C_e)^m}$
m	2.05	
R^2	0.96843	
χ^2	198.72	
Dubinin-Radushkevich		
Q_{DR}	208.19	
K_{DR}	809.11	$q_e = q_o\, e^{-K_{D-R}\, \varepsilon^2}$
E	0.02486	$\varepsilon = RTln(1 + \frac{1}{C_e})$
R^2	0.92931	
	381.39	$E = \frac{1}{\sqrt{2K_{DR}}}$
χ^2		

3.2.2. Kinetic study

The adsorption kinetics were examined to look into the rate of adsorption and any potential rate-controlling steps of adsorbents. Fig. 8 illustrates the fitting curves obtained using the pseudo-first-order [45], pseudo-second-order [46], Elovich [47] and intraparticle diffusion models. The Table 2 summarizes the parameters acquired from these models and their equations. The outcomes demonstrated that, with the initial concentration of 50 mg/L, DHPM reached adsorption equilibrium for MB within 150 min. Compared to other kinetic models, pseudo-second-order model demonstrated the lowest chi square ($\chi 2$) value, a coefficient of determination (R2) greater than 0.999 and qt,cal is close to qt,exep value. Therefore, the experimental data for adsorbing MB fits the pseudo-first-order model well, suggesting that diffusion is the process that regulates the rate. While the pseudo-second-order models were useful in characterizing the process of adsorption, but the diffusion mechanism was unable to determine [39]. Therefore, the intraparticle diffusion model was employed. Fig. 7 demonstrates that the rate constants can be obtained from the slope of the linear section of each curve. Additionally, the intercepts C can be obtained by extrapolating the first step in the curves to the time axis. The presence of two slopes in each curve suggests that there was a minimum of two diffusion steps involved in the adsorption process. The initial step corresponded to external surface adsorption or diffusion in macro-pores, which continued until the exterior surface reached saturation. The MB molecules penetrated less accessible pores, resulting in increased diffusion resistance and decreased diffusion rate. The magnitude of the slope of the linear portion reflected the diffusion rate, with a higher k indicating a faster diffusion process. Therefore, kp1 > kp2 indicated a reduction in the available free path for diffusion and a decrease in pore dimensions, leading to a slower diffusion rate [48]. The second step involved gradual adsorption, which was controlled by intraparticle diffusion.

Table 2. Kinetics parameters for adsorption of MB onto DHPM.

Model	Parameter value	Equation
$q_{t,exep}$ at 420 min	53.70	$q_t = \frac{C_o - C_t}{m} \times V$
PFO Model		
$q_{e,\,cal}$	50.07	
k_1	0.03737	$q_t = q_e(1 - e^{-K_1 t})$
R^2	0.9415	
χ^2	11.14	
PSO Model		
$q_{t,\,cal}$	55.58	
K_2	0.0009	$q_t = \frac{q_2^2 k_2 t}{1 + q_e K_2\, t}$
R^2	0.99992	
χ^2	1.49081	
Elovich		
α	12.18	
β	0.11158	$q_t = \frac{1}{\beta}\ln(1 + \alpha\beta t)$
R^2	0.97295	
χ^2	5.15	
Intraparticle diffusion Model		
$K_{p(1)}$	7.00	
C	4.68	$q_t = K_p\, t^{0.5} + C$
R^2	0.99444	
$K_{p(2)}$	0.67094	
C	40.40	
R^2	0.92471	

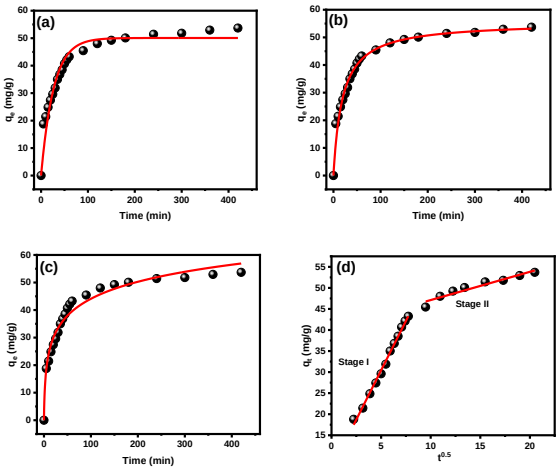

Fig 7. Nonlinear kinetic plot for the adsorption of MB on the DHPM (a) pseudo-first-order, (b) pseudo-second-order, (c) Elovich and (d) intraparticle diffusion models.

3.2.3. Thermodynamic study

In order to avail a better interpretation of the adsorption of MB onto DHPM adsorbent, various thermodynamic parameters were calculated. These included the enthalpy change (ΔH°, expressed in KJ/mol), free energy change (ΔG°, expressed in KJ/mol), and entropy change (ΔS°, expressed in KJ/mol). The following equations were used for the calculations:

$$\Delta G° = -RTlnKc$$

$$\ln K_c = \frac{\Delta S^\circ}{R} - \frac{\Delta H^\circ}{RT}$$

Where, Kc is the thermodynamic equilibrium constant (L/mol). T is temperature (K). R is the universal gas constant (J/mol*K). Table 3 results reveals the various thermodynamic parameters for MB adsorption onto DHPM. The adsorption process was spontaneous at the tested temperature, since the ΔG° value is negative. The value of ΔH° was positive, suggesting that MB adsorption via DHPM was endothermic, which was consistent with the analysis of the adsorption isotherm. Moreover, the ΔS° positive value indicates that the randomness of the system increased as the adsorption proceeded [39].

Table 3. Thermodynamic parameters for the adsorption of MB dye.

Temperature (K)	△G° (KJ/mol)	△H° (KJ/mol)	△S° (J/mol)
298	-1.07		
313	-1.23	43.47	144.42
323	-2.45		

Based on the results of isothermal, kinetic and thermodynamic studies reveals that, the adsorption process of MB dye on DHPM is a physical process that depends on weak attractive forces such as hydrogen bonding, n-π-interaction and π-π interaction as shown in Fig. 8. The FTIR spectrum was taken after adsorption experiment. The dye adsorbed materials were filtered and dried at 40 ºC. The –NH stretching appeared at 3344 cm-1 for the synthesized material was slightly shifted to lower frequency at 3298 cm-1 which indicates that the hydrogen bonding between dye and organic material (Fig. 9).

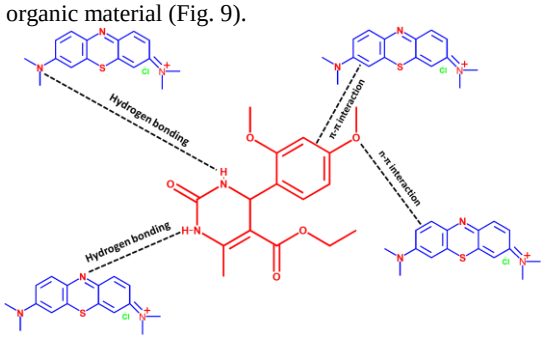

Fig. 8. Contribution forces in adsorption of MB dye on the surface of DHPM.

3.2.4. Recyclability of the present adsorbent

The repeated efficacy of the adsorbent in dye adsorption studies is essential for its long-term effectiveness. In order to evaluate the potential for reusing the suggested adsorbent, the self-assembled compound was added in a glass vial and the dye solutions (MB, 100 μg mL^{-1}) were then introduced to the vial. The dye solutions were analysed to determine their absorbance spectrum and the adsorption capability of MB dye was assessed. Afterwards, the self-assembled compounds were filtered off from the dye solution and subsequently washed with dil HCl/acetone mixture then with distilled water. Subsequently, a new dye solution was introduced and its absorbance was measured. After conducting five cycles, it was observed that the dye adsorption capacity for MB was decreased well with the initial cycle in Fig 10. These studies indicated that self-assembled compound have the potential to regenerate and selectively adsorb dyes for more times.

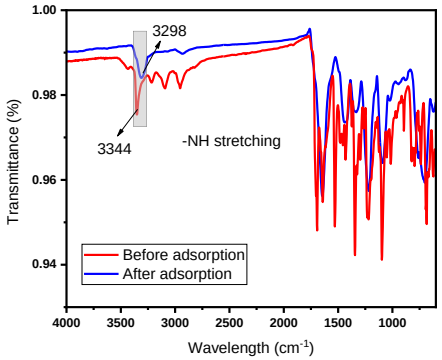

Fig 9. FT-IR for before and after adsorption of the material

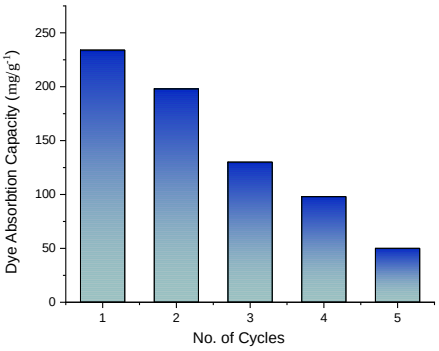

Fig. 10. Recyclability of the adsorbent over MB dye.

3.2.5. Comparisons of adsorption efficiency

The outcomes of our investigation with previous studies on the MB dye using different adsorbent materials were compared (Table 4). Among other conventionally synthesized composites or materials, the self-assembled compounds demonstrates the better adsorption capacity. From these results, the presently used material has a better vision in the adsorption field.

Table 4. Comparison of other adsorbents for removal of MB dye.

Adsorbent	Adsorption capacity q_m (mg g^{-1})	Isotherm model	pH	Temperature (K)	Equilibrium Time	References
NiO-HAp@ γ-Fe2O3	7.5	Langmuir	8.0	298	180 min	[49]
Modified biogenic HAp	205.22	Langmuir	7.0	313	240 min	[50]
Peanut shell	120.48	Langmuir	7.0	298	720 min	[51]
Kenaf core fibers	131.6	Langmuir	6.0	315	120 min	[52]
Peach stone	178.6	Langmuir	5.7	256	180 min	[53]
Pyrimidone derivative	234	Langmuir	9.0	298	180 min	Present study

4. Conclusion

A self-assembled bio-inspired heterocyclic compound synthesized using a green method employed as a novel effective adsorbent for the adsorptive removal of MB dye from aqueous solutions. Due to the ionisation of functional groups like keto and amine groups with increasing in temperature, the DHPM's adsorption ability towards MB enhanced in alkaline environments. The ideal adsorption conditions for MB are 0.1 g of adsorbate DHPM in 100 mL of a solution containing 50 mg L-1 of MB dye. Due to the hydrogen bonding, n-π and π-π interactions between the functional groups on the DHPM and MB, the adsorption capacity of DHPM for MB at 25^0C is 234 mg g-1. In kinetic studies, the PSO model is the most simulated to describe the MB dye adsorption kinetics as the intraparticle diffusion model indicates that the adsorption process takes place in two steps viz., surface diffusion and pore penetration. The non-linear Langmuir-Freundlich model were well fitted with the experimental equilibrium data. The thermodynamic analysis demonstrated that MB adsorption onto DHPM was endothermic ($\triangle H^o$: 43.47 KJ/mol^{-1}) and spontaneous ($\triangle G^o$: -1.07 KJ/mol^{-1} at 298 K). Overall, it can be concluded that DHPMs functions effectively as absorbents for adsorptive removal of cationic dye from aqueous solutions.

Declarations

Ethics Approval

All authors have read, understood, and have complied as applicable with the statement on "Ethical responsibilities of Authors" as found in the Instructions for Authors.

Funding

Self-Funded

Declaration of Competing Interest

The authors declare that they have no conflict of interest

Authors' contributions

Manojkumar Rajapriyan and Syed Ali Padusha M contributed to writing - the original draft, methodology, conceptualization, validation and investigation. Imran khan R, Meera Moydeen A, Badr M. Thamer and Abdulwahab Salah contributed to validation, data curation and formal analysis.

Availability of data and materials

All data analysed in this study are included in this article.

Acknowledgment

Author thanks to DST-FIST and DBT Star College Scheme (Government of India) for providing instrumentation facilities. Further, the author thank the PG & Research Department of Botany, Jamal Mohamed College (Autonomous), Tiruchirappalli-620 020 for extending their support to record the optical density.

Reference

[1] F. Raposo, M.A. De La Rubia, R. Borja, Methylene blue number as useful indicator to evaluate the adsorptive capacity of granular activated carbon in batch mode: Influence of adsorbate/adsorbent mass ratio and particle size, J. Hazard. Mater. 165 (2009) 291–299. https://doi.org/10.1016/j.jhazmat.2008.09.106.

[2] P. Singh, K. Sharma, V. Hasija, V. Sharma, S. Sharma, P. Raizada, M. Singh, A.K. Saini, A. Hosseini-Bandegharaei, V.K. Thakur, Systematic review on applicability of magnetic iron oxides–integrated photocatalysts for degradation of organic pollutants in water, Mater. Today Chem. 14 (2019) 100186. https://doi.org/10.1016/j.mtchem.2019.08.005.

[3] D. Ghosh, K.G. Bhattacharyya, Adsorption of methylene blue on kaolinite, Appl. Clay Sci. 20 (2002) 295–300. https://doi.org/10.1016/S0169-1317(01)00081-3.

[4] R. Ahmad, R. Kumar, Adsorption studies of hazardous malachite green onto treated ginger waste, J. Environ. Manage. 91 (2010) 1032–1038. https://doi.org/10.1016/j.jenvman.2009.12.016.

[5] Z. Wu, H. Zhong, X. Yuan, H. Wang, L. Wang, X. Chen, G. Zeng, Y. Wu, Adsorptive removal of methylene blue by rhamnolipid-functionalized graphene oxide from wastewater, Water Res. 67 (2014) 330–344. https://doi.org/10.1016/j.watres.2014.09.026.

[6] S.A. Ishak, M.F. Murshed, H. Md Akil, N. Ismail, S.Z. Md Rasib, A.A.S. Al-Gheethi, The Application of Modified Natural Polymers in Toxicant Dye Compounds Wastewater: A Review, Water. 12 (2020) 2032. https://doi.org/10.3390/w12072032.

[7] W. Wang, Y. Zhao, H. Bai, T. Zhang, V. Ibarra-Galvan, S. Song, Methylene blue removal from water using the hydrogel beads of poly(vinyl alcohol)-sodium alginate-chitosan-montmorillonite, Carbohydr. Polym. 198 (2018) 518–528. https://doi.org/10.1016/j.carbpol.2018.06.124.

[8] S. Wong, N. Ngadi, I.M. Inuwa, O. Hassan, Recent advances in applications of activated carbon from biowaste for wastewater treatment: A short review, J. Clean. Prod. 175 (2018) 361–375. https://doi.org/10.1016/j.jclepro.2017.12.059.

[9] L. Roshanfekr Rad, M. Anbia, Zeolite-based composites for the adsorption of toxic matters from water: A review, J. Environ. Chem. Eng. 9 (2021) 106088. https://doi.org/10.1016/j.jece.2021.106088.

[10] J.V. Fernandes, A.M. Rodrigues, R.R. Menezes, G. de A. Neves, Adsorption of Anionic Dye on the Acid-Functionalized Bentonite, Materials (Basel). 13 (2020) 3600. https://doi.org/10.3390/ma13163600.

[11] B. Ates, S. Koytepe, A. Ulu, C. Gurses, V.K. Thakur, Chemistry, Structures, and Advanced Applications of Nanocomposites from Biorenewable Resources, Chem. Rev. 120 (2020) 9304–9362. https://doi.org/10.1021/acs.chemrev.9b00553.

[12] A. Baimenov, D.A. Berillo, S.G. Poulopoulos, V.J. Inglezakis, A review of cryogels synthesis, characterization and applications on the removal of heavy metals from aqueous solutions, Adv. Colloid Interface Sci. 276 (2020) 102088. https://doi.org/10.1016/j.cis.2019.102088.

[13] W. Wan, A.D. Bannerman, L. Yang, H. Mak, Poly(Vinyl Alcohol) Cryogels for Biomedical Applications, in: 2014: pp. 283–321. https://doi.org/10.1007/978-3-319-05846-7_8.

[14] G. Balkız, E. Pingo, N. Kahya, H. Kaygusuz, F. Bedia Erim, Graphene Oxide/Alginate Quasi-Cryogels for Removal of Methylene Blue, Water, Air, Soil Pollut. 229 (2018) 131. https://doi.org/10.1007/s11270-018-3790-5.

[15] M. Chen, Y. Shen, L. Xu, G. Xiang, Z. Ni, Highly efficient and rapid adsorption of methylene blue dye onto vinyl hybrid silica nano-cross-linked nanocomposite hydrogel, Colloids Surfaces A Physicochem. Eng. Asp. 613 (2021) 126050. https://doi.org/10.1016/j.colsurfa.2020.126050.

[16] S. Soni, P.K. Bajpai, J. Mittal, C. Arora, Utilisation of cobalt doped Iron based MOF for enhanced removal and recovery of methylene blue dye from waste water,

J. Mol. Liq. 314 (2020) 113642. https://doi.org/10.1016/j.molliq.2020.113642.

[17] V. Kumar, P. Saharan, A.K. Sharma, A. Umar, I. Kaushal, A. Mittal, Y. Al-Hadeethi, B. Rashad, Silver doped manganese oxide-carbon nanotube nanocomposite for enhanced dye-sequestration: Isotherm studies and RSM modelling approach, Ceram. Int. 46 (2020) 10309–10319. https://doi.org/10.1016/j.ceramint.2020.01.025.

[18] L. Wang, J. Zhang, A. Wang, Removal of methylene blue from aqueous solution using chitosan-g-poly(acrylic acid)/montmorillonite superadsorbent nanocomposite, Colloids Surfaces A Physicochem. Eng. Asp. 322 (2008) 47–53. https://doi.org/10.1016/j.colsurfa.2008.02.019.

[19] V.P. Kasperchik, A.L. Yaskevich, A. V. Bil'dyukevich, Wastewater treatment for removal of dyes by coagulation and membrane processes, Pet. Chem. 52 (2012) 545–556. https://doi.org/10.1134/S0965544112070079.

[20] Y.-H. Chiu, T.-F. Chang, C.-Y. Chen, M. Sone, Y.-J. Hsu, Mechanistic Insights into Photodegradation of Organic Dyes Using Heterostructure Photocatalysts, Catalysts. 9 (2019) 430. https://doi.org/10.3390/catal9050430.

[21] C.-Z. Liang, S.-P. Sun, F.-Y. Li, Y.-K. Ong, T.-S. Chung, Treatment of highly concentrated wastewater containing multiple synthetic dyes by a combined process of coagulation/flocculation and nanofiltration, J. Memb. Sci. 469 (2014) 306–315. https://doi.org/10.1016/j.memsci.2014.06.057.

[22] P. Senthil Kumar, G.J. Joshiba, C.C. Femina, P. Varshini, S. Priyadharshini, M.S. Arun Karthick, R. Jothirani, A critical review on recent developments in the low-cost adsorption of dyes from wastewater, Desalin. WATER Treat. 172 (2019) 395–416. https://doi.org/10.5004/dwt.2019.24613.

[23] J. Joseph, R.C. Radhakrishnan, J.K. Johnson, S.P. Joy, J. Thomas, Ion-exchange mediated removal of cationic dye-stuffs from water using ammonium phosphomolybdate, Mater. Chem. Phys. 242 (2020) 122488. https://doi.org/10.1016/j.matchemphys.2019.122488.

[24] M.C. Collivignarelli, A. Abbà, M. Carnevale Miino, S. Damiani, Treatments for color removal from wastewater: State of the art, J. Environ. Manage. 236 (2019) 727–745. https://doi.org/10.1016/j.jenvman.2018.11.094.

[25] A. Mittal, R. Ahmad, I. Hasan, Iron oxide-impregnated dextrin nanocomposite: synthesis and its application for the biosorption of Cr(VI) ions from aqueous solution, Desalin. Water Treat. 57 (2016) 15133–15145. https://doi.org/10.1080/19443994.2015.1070764.

[26] A. Mittal, D. Kaur, J. Mittal, Batch and bulk removal of a triarylmethane dye, Fast Green FCF, from wastewater by adsorption over waste materials, J. Hazard. Mater. 163 (2009) 568–577. https://doi.org/10.1016/j.jhazmat.2008.07.005.

[27] H.A. Altaleb, B.M. Thamer, M.M. Abdulhameed, H. El-Hamshary, S.Z. Mohammady, A.M. Al-Enizi, Efficient electrospun terpolymer nanofibers for the removal of cationic dyes from polluted waters: A non-linear isotherm and kinetic study, J. Environ. Chem. Eng. 9 (2021) 105361. https://doi.org/10.1016/j.jece.2021.105361.

[28] B.M. Thamer, A. Aldalbahi, M. Moydeen A., M.H. El-Newehy, In Situ Preparation of Novel Porous Nanocomposite Hydrogel as Effective Adsorbent for the Removal of Cationic Dyes from Polluted Water, Polymers (Basel). 12 (2020) 3002. https://doi.org/10.3390/polym12123002.

[29] B.M. Thamer, A. Aldalbahi, M. Moydeen A, A.M. Al-Enizi, H. El-Hamshary, M.H. El-Newehy, Fabrication of functionalized electrospun carbon nanofibers for enhancing lead-ion adsorption from aqueous solutions, Sci. Reports 2019 91. 9 (2019) 1–15. https://doi.org/10.1038/s41598-019-55679-6.

[30] B.M. Thamer, A. Aldalbahi, M. Moydeen A, M. Rahaman, M.H. El-Newehy, Modified Electrospun Polymeric Nanofibers and Their Nanocomposites as Nanoadsorbents for Toxic Dye Removal from Contaminated Waters: A Review, Polymers (Basel). 13 (2020) 20. https://doi.org/10.3390/polym13010020.

[31] V.K. Gupta, S. Agarwal, R. Ahmad, A. Mirza, J. Mittal, Sequestration of toxic congo red dye from aqueous solution using ecofriendly guar gum/ activated carbon nanocomposite., Int. J. Biol. Macromol. 158 (2020) 1310–1318. https://doi.org/10.1016/j.ijbiomac.2020.05.025.

[32] R. Ahmad, I. Hasan, A. Mittal, Adsorption of Cr(VI) and Cd(II) on chitosan grafted polyaniline-OMMT nanocomposite: isotherms, kinetics and thermodynamics studies, Desalin. WATER Treat. 58 (2017) 144–153. https://doi.org/10.5004/dwt.2017.0414.

[33] S.K. Sharma, ed., Green Chemistry for Dyes Removal from Wastewater, Wiley, 2015. https://doi.org/10.1002/9781118721001.

[34] J. Lehn, Supramolecular Chemistry, Wiley, 1995. https://doi.org/10.1002/3527607439.

[35] G.M. Whitesides, B. Grzybowski, Self-Assembly at All Scales, Science (80-.). 295 (2002) 2418–2421. https://doi.org/10.1126/science.1070821.

[36] S. Zhang, Fabrication of novel biomaterials through molecular self-assembly, Nat. Biotechnol. 21 (2003) 1171–1178. https://doi.org/10.1038/nbt874.

[37] K. Takazawa, Y. Kitahama, Y. Kimura, G. Kido, Optical Waveguide Self-Assembled from Organic Dye Molecules in Solution, Nano Lett. 5 (2005) 1293–1296. https://doi.org/10.1021/nl050469y.

[38] M.G. Dekamin, F. Mehdipoor, A. Yaghoubi, 1,3,5-Tris(2-hydroxyethyl)isocyanurate functionalized graphene oxide: a novel and efficient nanocatalyst for the one-pot synthesis of 3,4-dihydropyrimidin-2(1H)-ones, New J. Chem. 41 (2017) 6893–6901. https://doi.org/10.1039/C7NJ00632B.

[39] B.M. Thamer, H. El-Hamshary, S.S. Al-Deyab, M.H. El-Newehy, Functionalized electrospun carbon nanofibers for removal of cationic dye, Arab. J. Chem. 12 (2019) 747–759. https://doi.org/10.1016/j.arabjc.2018.07.020.

[40] I. Langmuir, THE ADSORPTION OF GASES ON PLANE SURFACES OF GLASS, MICA AND PLATINUM., J. Am. Chem. Soc. 40 (1918) 1361–1403. https://doi.org/10.1021/ja02242a004.

[41] pp. 385–471. Freundlich, H.M.F., Over the adsorption in solution, Z. Phys. Chem., 1906, vol. 57, No Title, (n.d.).

[42] 1947. Equation of the characteristic Dubinin, M., Radushkevich, L., 875–890. curve of activated charcoal. Chem. Zentr 1, No Title, (n.d.).

[43] R. Sips, Combined form of Langmuir and Freundlich equations, J. Chem. Phys. (1948).
[44] B.M. Thamer, A.A. Shaker, M.M. Abdul Hameed, A.M. Al-Enizi, Highly selective and reusable nanoadsorbent based on expansive clay-incorporated polymeric nanofibers for cationic dye adsorption in single and binary systems, J. Water Process Eng. 54 (2023) 103918. https://doi.org/10.1016/j.jwpe.2023.103918.
[45] S. (1898) A. the T. of S.-C.A. of S.S. Lagergren, 1-39. Kungliga Svenska Vetenskapsakademiens Handlingar , 24, No Title, (n.d.).
[46] Y.S. Ho, D.A.J. Wase, C.F. Forster, Kinetic Studies of Competitive Heavy Metal Adsorption by Sphagnum Moss Peat, Environ. Technol. 17 (1996) 71–77. https://doi.org/10.1080/09593331708616362.
[47] S.H. Chien, W.R. Clayton, Application of Elovich Equation to the Kinetics of Phosphate Release and Sorption in Soils, Soil Sci. Soc. Am. J. 44 (1980) 265–268. https://doi.org/10.2136/sssaj1980.03615995004400020013x.
[48] C. (Sage) Cheng, J. Deng, B. Lei, A. He, X. Zhang, L. Ma, S. Li, C. Zhao, Toward 3D graphene oxide gels based adsorbents for high-efficient water treatment via the promotion of biopolymers, J. Hazard. Mater. 263 (2013) 467–478. https://doi.org/10.1016/j.jhazmat.2013.09.065.
[49] A. Phasuk, S. Srisantitham, T. Tuntulani, W. Anutrasakda, Facile synthesis of magnetic hydroxyapatite-supported nickel oxide nanocomposite and its dye adsorption characteristics, Adsorption. 24 (2018) 157–167. https://doi.org/10.1007/s10450-017-9931-0.
[50] G. Wang, L. Yang, L. Jiang, M. Shi, Z. Wei, W. Zhong, S. Li, J. Cui, W. Wei, Simple combination of humic acid with biogenic hydroxyapatite achieved highly efficient removal of methylene blue from aqueous solution, RSC Adv. 6 (2016) 67888–67897. https://doi.org/10.1039/C6RA08715A.
[51] P. Wang, Q. Ma, D. Hu, L. Wang, Adsorption of methylene blue by a low-cost biosorbent: citric acid modified peanut shell, Desalin. Water Treat. 57 (2016) 10261–10269. https://doi.org/10.1080/19443994.2015.1033651.
[52] M.S. Sajab, C.H. Chia, S. Zakaria, S.M. Jani, M.K. Ayob, K.L. Chee, P.S. Khiew, W.S. Chiu, Citric acid modified kenaf core fibres for removal of methylene blue from aqueous solution, Bioresour. Technol. 102 (2011) 7237–7243. https://doi.org/10.1016/j.biortech.2011.05.011.
[53] N. Thomas, D.D. Dionysiou, S.C. Pillai, Heterogeneous Fenton catalysts: A review of recent advances, J. Hazard. Mater. 404 (2021) 124082. https://doi.org/10.1016/j.jhazmat.2020.124082.